

Improving Resistance to Adversarial Deformations by Regularizing Gradients

Pengfei Xia and Bin Li

CAS Key Laboratory of Technology in Geo-spatial Information Processing and Application Systems
Department of Electronic Engineering and Information Science
University of Science of Technology of China
Hefei, China
binli@ustc.edu.cn

Abstract

Improving the resistance of deep neural networks against adversarial attacks is important for deploying models to realistic applications. Currently, most defense methods are designed to defend against additive noise attacks, their performance cannot be guaranteed when against non-additive noise attacks. In this paper, we focus on adversarial deformations, a typical class of non-additive noise attacks, and propose a flow gradient regularization with random start to improve the resistance of models. Theoretically, we prove that, compared with input gradient regularization, regularizing flow gradients is able to get a tighter bound.

Across multiple datasets, architectures, and adversarial deformations, our experimental results consistently indicate that models trained with flow gradient regularization can acquire a better resistance than trained with input gradient regularization with a large margin. Moreover, compared with adversarial training, our method can achieve better results in optimization-based and gradient-free attacks, and combining these two methods can improve the resistance against deformation attacks further. Finally, we give a unified form of gradient regularization, which can be used to derive the corresponding form when facing other types of attack.

Introduction

Deep neural networks (DNNs), especially convolutional neural networks (CNNs), have achieved remarkable success in computer vision tasks (Krizhevsky, Sutskever, and Hinton 2012; Simon-Gabriel et al. 2019; Girshick 2015; Long, Shelhamer, and Darrell 2015). However, small, imperceptible changes to the underlying images can easily fool DNNs (Szegedy et al. 2013; Goodfellow, Shlens, and Szegedy 2014). Such modified inputs, also known as *adversarial examples*, pose a doubt when applying deep learning models to security-sensitive applications, such as face recognition, surveillance, and self-driving cars (Sharif et al. 2016; Heaven 2019).

Under the criterion that the instances with or without perturbations should look similar, there are many ways to perform such changes. The most intuitive and widely concerned one is to add a crafted noise to the original image, where

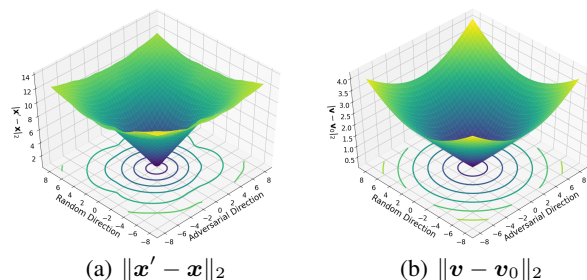


Figure 1: Calculating $\|\mathbf{x}' - \mathbf{x}\|_2$ and $\|\mathbf{v} - \mathbf{v}_0\|_2$ along a random direction and the adversarial direction generated by stAdv on CIFAR-10.

the l_p -norm of the noise is limited to a small value to ensure imperceptible to human vision (Goodfellow, Shlens, and Szegedy 2014; Madry et al. 2017; Carlini and Wagner 2017). In addition to additive noise attacks described above, researchers have been working to find other ways to cheat deep models. For example, Engstrom et al. (2017) constructed adversarial examples by rotating and translating images. Xiao et al. (2018b) proposed stAdv, which attacks models by shifting the spatial position of each pixel. Brown et al. (2017) created adversarial image patches that can fool classifiers in the real world. The diversity in adversarial examples imposes great challenges to the research on building adversarial robust models.

Improving resistance to adversarial attacks is important for deploying DNNs to realistic applications. In order to achieve this goal, many defenses have come into the scene, such as adversarial training (Goodfellow, Shlens, and Szegedy 2014; Madry et al. 2017; Wang and Zhang 2019), feature squeezing (Xu, Evans, and Qi 2017), input gradient regularization (Ross and Doshi-Velez 2018; Jakubovitz and Giryas 2018; Chan et al. 2019) and certified defenses (Hein and Andriushchenko 2017; Raghuathan, Steinhardt, and Liang 2018). One concern is that these defenses mostly focus on additive noise attacks, and their resistance to other types cannot be guaranteed (Engstrom et al. 2017; Xiao et al. 2018b). How to defense non-additive noise attacks needs more attention.

In this paper, we focus on improving the resistance of

models against adversarial deformations (Xiao et al. 2018b; Alaifari, Alberti, and Gauksson 2018), a typical class of non-additive noise attacks. Unlike additive noise attacks, which fool deep models by perturbing the intensity of each pixel, adversarial deformations flow the position of each pixel in clean images. Despite resulting in large l_p -norm distance, the generated image can maintain high perceptual quality (Xiao et al. 2018b).

To resist such deformations, the main principle we follow is that the output of a robust model should be insensitive to a small variation of input, where the key issue is to design a suitable metric to evaluate the variation. Defensive methods adopting the same principle, such as input gradient regularization (Lyu, Huang, and Liang 2015; Ross and Doshi-Velez 2018) and Jacobians regularization (Jakubovitz and Giryes 2018; Hoffman, Roberts, and Yaida 2019), use l_p -norm of the difference between the adversarial image \mathbf{x}' and the clean image \mathbf{x} , $\|\mathbf{x}' - \mathbf{x}\|_p$, to evaluate the variation. For additive noise attacks, it is a good and effective measure. However, it is not completely suitable for adversarial deformations, as shown in Figure 1(a), where a shorter direction exists to result in a large l_p -norm distance, thus leads to those defenses built on $\|\mathbf{x}' - \mathbf{x}\|_p$ are less effective in defending against adversarial deformations. It is worth noting that we only show two directions and in the real high-dimensional space, the situation will be sharper.

Let us first revisit the form of generating adversarial deformations (Xiao et al. 2018b; Alaifari, Alberti, and Gauksson 2018). Given a clean image \mathbf{x} , an adversary \mathbf{x}' is constructed by $\mathbf{x}' = \mathcal{I}(\mathbf{x}, \mathbf{v})$, where \mathcal{I} is the bilinear interpolation function and \mathbf{v} is the flow matrix that indicates the offset of each pixel position. The **pointwise slope** and the **piecewise linear** introduced in the process of constructing adversarial deformations, which will be detailed in the following section, are the main reasons for the above phenomenon. Namely, these two characteristics lead to the incorrect estimation of the input variation by the methods built on $\|\mathbf{x}' - \mathbf{x}\|_p$, and finally lead to the discounted defense effect.

In order to effectively protect deep models from adversarial deformations, in this paper, we propose a flow gradient regularization (FGR) with random start (RS) to reduce the output sensitivity to the small variation of input. First of all, instead of $\|\mathbf{x}' - \mathbf{x}\|_p$, our method evaluate the variation by directly calculate the degree of position flow, i.e., $\|\mathbf{v} - \mathbf{v}_0\|_p$, where \mathbf{v}_0 is the identity value so that $\mathbf{x} = \mathcal{I}(\mathbf{x}, \mathbf{v}_0)$, and is able to model the pointwise slope of deformations. Secondly, random start technique is adopted to increase the ability of FGR to reflect the piecewise linear.

The main contributions of this paper can be summarized below:

- In this paper, we analyze the defects of using $\|\mathbf{x}' - \mathbf{x}\|_p$ to measure the variation of adversarial deformations, and suggest to directly use $\|\mathbf{v} - \mathbf{v}_0\|_p$ instead;
- Based on $\|\mathbf{v} - \mathbf{v}_0\|_p$, a flow gradient regularization with random start is proposed to improve the resistance to adversarial deformations. Theoretically, we prove that regularizing flow gradients is able to acquire a tighter bound

than regularizing input gradients;

- Our experiments results consistently show that training with FGR performs better than training with IGR (input gradient regularization) with a large margin when against deformations generated in four methods. Moreover, FGR is better than adversarial training in optimization-based and gradient-free attacks, while these two methods can still be combined to improve resistance further;
- We discuss the ways to apply gradient regularization methods against other types of attack, and give a unified formulation of the problem.

Related Work

Adversarial Attacks

Since Szegedy et al. (2013) first noticed the existence of adversarial examples, many methods have been proposed for enhancing such attacks. Goodfellow et al. (2014) provided a linear explanation of adversarial examples and proposed a single-step attack named Fast Gradient Sign Method (FGSM). Subsequently, some works have been done to expand it to multiple steps (Kurakin, Goodfellow, and Bengio 2016; Dong et al. 2018; Xie et al. 2017). Among them, Projected Gradient Descend (PGD) proposed by Madry et al. (2017) is the most typical and shows a strong attack ability. Carlini and Wagner (Carlini and Wagner 2017) proposed C&W attack, a powerful approach that regards generating adversarial examples as an optimization problem. Some works (Xiao et al. 2018a; Song et al. 2018) construct an adversary by generative adversarial networks. Nowadays, building more aggressive and more diverse attacks is still a hot topic (Chen et al. 2018; Ru et al. 2019; Croce and Hein 2019; Croce and Hein 2020). Attacks mentioned above mostly adopt the same form to construct adversarial examples, i.e., adding a crafted noise to the clean image, and limiting $\|\mathbf{x}' - \mathbf{x}\|_p$ to be a small value to guarantee visual similarity. These attacks refer to as additive noise attacks.

Besides additive noise attacks, there are some works performing such chicaneries in different ways, and we collectively call it as non-additive noise attacks. One typical is adversarial deformations, which fools deep models by flowing the position of each pixel in the input image. Xiao et al. (2018b) first introduced this type of attack and proposed stAdv to find a suitable adversary. Alaifari et al. (2018) presented a method to find similar adversarial examples with a first-order optimizer. Zhang et al. (2019) combined both spatial and pixel perturbations and proposed a joint adversarial attack. In general, adversarial examples generated in this way are more imperceptible for humans, and the resistance of defenses designed for additive noise attacks cannot be guaranteed.

The non-additive noise family also includes some other attack methods. Engstrom et al. (2017) found that neural networks are vulnerable to simple image transformations, such as rotation and translation. Brown et al. (2017) created universal, robust, targeted image patches that can fool classifiers in the real world. Sharif et al. (2016; 2017) fooled a face recognition system by wearing elaborate glasses on face

images. Qiu et al. (2019) proposed SemanticAdv to generate adversarial examples by editing semantic information, such as the color of hair. Afifi et al. (2019) explored that incorrect white balance adjustment negatively impacts the performance of DNNs.

The diversity in generating methods for adversarial samples imposes great challenges to the research on constructing adversarial robust models.

Adversarial Defenses

To improve resistance of models to such attacks, extensive efforts have come into the scene, such as preprocessing (Gu and Rigazio 2014; Xie et al. 2017; Kou et al. 2019), feature squeezing (Xu, Evans, and Qi 2017), model ensemble (Tramèr et al. 2017; Sen, Ravindran, and Raghunathan 2020) and certified defenses (Raghunathan, Steinhardt, and Liang 2018). The most direct and effective defenses so far are training models with generated examples as a kind of data augmentation. These adversarial training methods are first introduced by Goodfellow et al. (2014) and developed by Madry et al. (2017). Subsequently, research continued to be presented. Some works (Shafahi et al. 2019; Zhang et al. 2019) tried to decrease time consumption, which is one of the major drawbacks of adversarial training. Tramèr and Boneh (Tramèr and Boneh 2019) developed it to defense both l_1 , l_2 and l_∞ attacks simultaneously.

The main idea of another type of defenses is to decrease the sensitivity of models' output to a small variation of input. Among them, the most typical methods are input gradient regularization (Lyu, Huang, and Liang 2015; Ross and Doshi-Velez 2018) and Jacobians regularization (Jakubovitz and Giryes 2018), where both are adding penalty items to the loss function during model training. Hoffman et al. (2019) developed an efficient approximate algorithm to implement Jacobians regularizer. Chan et al. (2019) proposed Jacobian adversarially regularized network (JARN) to improve the saliency of Jacobians, and further increase robustness.

These methods are mainly designed for additive noise attacks, and their resistance to other types of attack are less effective. Engstrom et al. (2017) showed that l_∞ -bounded adversarial training actually damages the accuracy of models to adversarial rotations and translations. Xiao et al. (2018b) tested different defenses against adversarial deformations and found that these methods can only achieve low defense performance.

How to defense non-additive attacks needs further research.

Preliminaries

Adversarial Examples

Given a deep model f , the aim of attack methods is to find an adversarial example \mathbf{x}' so that $f(\mathbf{x}') \neq f(\mathbf{x})$ for untargeted attack or $f(\mathbf{x}') = \mathbf{t}$ for targeted attack. The most common form is adding a crafted noise δ to the clean image \mathbf{x} , i.e., $\mathbf{x}' = \mathbf{x} + \delta$. After determining the form of attack, researches mainly focus on how to find a suitable δ . In this paper, we review four types, single-step attack, multi-step attack, optimization-based attack, and gradient-free attack,

which are also used to generate adversarial deformations in our experiments.

Single-step attack (FGSM (Goodfellow, Shlens, and Szegedy 2014)) uses a single gradient ascent step to construct adversarial examples

$$\mathbf{x}' = \mathbf{x} + \epsilon \cdot \text{sign}(\nabla_{\mathbf{x}} \mathcal{L}(\mathbf{x}, \mathbf{y})), \quad (1)$$

where \mathcal{L} is the loss function, \mathbf{y} is the one-hot groundtruth label and ϵ is a small value that specifying a noise budget.

Multi-step attack (BIM (Kurakin, Goodfellow, and Bengio 2016), PGD (Madry et al. 2017)) is an extension of single-step that generating an adversary by iteratively calculating

$$\mathbf{x}^{k+1} = \text{clip}(\mathbf{x}^k + \alpha \cdot \text{sign}(\nabla_{\mathbf{x}^k} \mathcal{L}(\mathbf{x}^k, \mathbf{y}))), \quad (2)$$

where α is the step size, clip is the clip function to ensure that \mathbf{x}^{k+1} is within a reasonable range, $\mathbf{x}^0 = \mathbf{x}$, $\mathbf{x}' = \mathbf{x}^K$ and K is the total number of iterations.

Optimization-based attack (L-BFGS (Szegedy et al. 2013), C&W (Carlini and Wagner 2017)) produces an adversary for target \mathbf{t} by minimizing the formulation

$$\mathcal{L}(\mathbf{x} + \delta, \mathbf{t}) + c \cdot \|\delta\|_p, \quad (3)$$

where c is a chosen constant that balancing the strength and the imperceptibility.

Unlike the above three attacks, which all use gradient information, gradient-free attack (ZOO (Chen et al. 2017), One Pixel (Su, Vargas, and Sakurai 2019)) only need the classification confidence of models, and search δ by gradient estimation or evolutionary algorithm.

Adversarial Deformations

As shown in Figure 2, we briefly introduce adversarial deformations, a typical class of non-additive noise attacks. Assuming the clean image $\mathbf{x} \in \mathbb{R}^{W \times H \times C}$ with width W , height H and C channels, $\mathbf{g} = \{(m_i, n_i)\}_{i=1, \dots, W \times H} \in \mathbb{R}^{W \times H \times 2}$ is a 2D grid to denote the location of each pixel. Adversarial deformations fool deep models by defining a flow matrix to shift the location of each pixel, $\mathbf{v} = \{(\Delta m_i, \Delta n_i)\}_{i=1, \dots, W \times H} \in \mathbb{R}^{W \times H \times 2}$. \mathcal{I} is the bilinear interpolation function, and the adversarial example is generated by $\mathbf{x}' = \mathcal{I}(\mathbf{x}, \mathbf{g} + \mathbf{v})$, where the i -th pixel of \mathbf{x}' is calculated as below,

$$\mathbf{x}'_i = \sum_{q \in NB(m'_i, n'_i)} \mathbf{x}_q (1 - |m'_i - m_q|)(1 - |n'_i - n_q|), \quad (4)$$

where $m'_i = m_i + \Delta m_i$, $n'_i = n_i + \Delta n_i$ are the shifted location, $NB(m'_i, n'_i)$ are the indices of the 4-pixel neighbors at location (m'_i, n'_i) . In the following writing, we omit \mathbf{g} and use $\mathbf{x}' = \mathcal{I}(\mathbf{x}, \mathbf{v})$ for simplicity.

Finding a feasible \mathbf{v} is similar to finding δ in additive noise attacks, and can be solved with the four methods mentioned above. For more details about adversarial deformations, please refer to (Xiao et al. 2018a; Alaifari, Alberti, and Gauksson 2018).

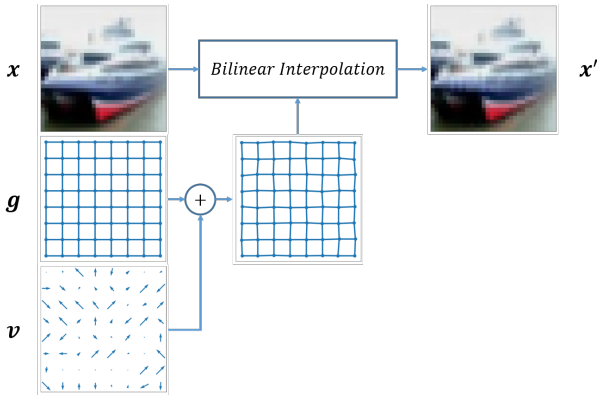


Figure 2: The process of generating adversarial deformations.

Input Gradient Regularization

Input gradient regularization (Ross and Doshi-Velez 2018) influences the training process by adding $\|\nabla_x \mathcal{L}(x, y)\|_p$ as the penalty item to reduce the sensitivity of output to the input variation, i.e.,

$$\text{Loss} = \mathcal{L}(x, y) + \lambda \cdot \|\nabla_x \mathcal{L}(x, y)\|_q, \quad (5)$$

where λ is a hyperparameter that controls the penalty strength.

Adversarial Training

Adversarial training improves robustness by optimizing

$$\arg \min_{\theta} \mathbb{E}_{(x, y)} \left[\max_{\|\delta\|_p \leq \epsilon} \mathcal{L}_{\theta}(x + \delta, y) \right], \quad (6)$$

where θ is the network parameter.

Methodology

For a robust classifier, the output should be insensitive to the small variation of input (Lyu, Huang, and Liang 2015; Simon-Gabriel et al. 2019), where the key issue is how to measure the small variation of input. Many methods have been proposed to achieve the goal, like regularizing the Frobenius norm of the Jacobian matrix of models evaluated on the output data (Jakubovitz and Giryes 2018; Hoffman, Roberts, and Yaida 2019). However, the l_p -norm distance in input space, i.e., $\|x' - x\|_p$, used in the previous works is not entirely suitable for measuring adversarial deformations.

In this section, we first elaborate some of the shortcomings of $\|x' - x\|_p$ when measuring the small variation of adversarial deformations and try to give some explanation on the possible reasons. Then, a flow gradient regularization with random start is proposed to improve the resistance of models against such attacks.

Defects Analysis

There are some defects appear when utilizing $\|x' - x\|_p$ to evaluate the deformations, as shown in Figure 1(a), where the value is calculated along a random flow matrix and

the adversarial flow matrix generated by stAdv (Xiao et al. 2018b). The surface indicates the defects: (1) the rising rate of $\|x' - x\|_p$ changes in different directions, and (2) local distortions appear on the surface. One of the consequences these might bring is that defenses based on $\|x' - x\|_p$ are less effective in defending against adversarial deformations, because a shorter direction exists to result in a large l_p -norm distance.

But why do these situations happens? Revisiting the form of generating adversarial deformations, $x' = \mathcal{I}(x, v)$, we can acquire some clues. First of all, for the i -th pixel in the image, the slope of $|x'_i - x_i|$, i.e., $\frac{\partial |x'_i - x_i|}{\partial v_i}$, is decided by the 4-pixel neighbors at location (m'_i, n'_i) (see Equation 4), which is called pointwise slope. Namely, for different pixels, the slope of $\mathcal{I}(x, v)$ is different, which causes $\|x' - x\|_p$ has a larger rising rate in some directions. Secondly, the cause of surface distortions is that, with the change of v , for any pixel, $\mathcal{I}(x, v)$ exhibits piecewise linear.

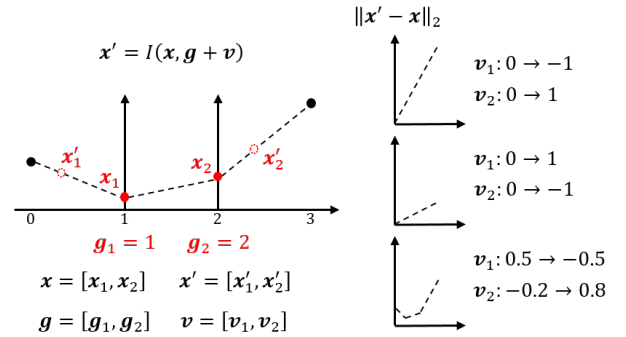


Figure 3: An example of $\mathcal{I}(x, v)$, where the red dots are x_1 and x_2 , black dots are nearest neighbors, and x'_i is generated by linear interpolation controlled by v_i between x_i and one of neighbors.

An example in 1D is shown in Figure 3 for a better explanation about pointwise slope and piecewise linear. Considering $x = [x_1, x_2]$ denotes the clean sample, $x' = [x'_1, x'_2]$ denotes the adversarial instance, $g = [g_1 = 1, g_2 = 2]$ denotes the normal location grid, and $v = [v_1, v_2]$ denotes the flow matrix. Pointwise slope means that when v_i moving the same distance, $|x'_i - x_i|$ is different for each point. This leads to a faster rising rate of $\|x' - x\|_p$ in some directions, such as flowing $\{v_1 : 0 \rightarrow -1, v_2 : 0 \rightarrow 1\}$ obviously causes a greater $\|x' - x\|_p$ than $\{v_1 : 0 \rightarrow 1, v_2 : 0 \rightarrow -1\}$. Piecewise means for each point, $|x'_i - x_i|$ is a piecewise linear function, and eventually causes $\|x' - x\|_p$ to appear non-linear, as $\{v_1 : 0.5 \rightarrow -0.5, v_2 : -0.2 \rightarrow 0.8\}$ shown in Figure 3.

In order to effectively defend against adversarial deformations, the method proposed in this paper is designed with the above two characteristics considered.

Flow Gradient Regularization

First, we consider to evaluate the small variation by using $\|v - v_0\|_p$ instead of $\|x' - x\|_p$, and derive that regulariz-

ing the flow gradients can improve the resistance against adversarial deformations. Essentially, compared to input gradient regularization, flow gradient regularization introduces the modeling of the pointwise slope, and is able to obtain a tighter bound.

The overall principle is that the output of models should be insensitive to small variation of the input. Defining $\mathcal{L}(\mathbf{x}, \mathbf{y})$ as a loss of the model f , and \mathbf{x} is the input image and \mathbf{y} is the one-hot groundtruth label respectively. Suppose $\delta\mathcal{L}$ is a variation of the loss, that is

$$\delta\mathcal{L} = |\mathcal{L}(\mathbf{x}', \mathbf{y}) - \mathcal{L}(\mathbf{x}, \mathbf{y})|. \quad (7)$$

If taking $\|\mathbf{x}' - \mathbf{x}\|_p$ as the variation metric, we can directly perform Taylor expansion on $\mathcal{L}(\mathbf{x}', \mathbf{y})$ around point \mathbf{x} , and derive the form of input gradient regularization (Ross and Doshi-Velez 2018). Instead, we use $\|\mathbf{v} - \mathbf{v}_0\|_p$ in this paper. Substituting $\mathbf{x}' = \mathcal{I}(\mathbf{x}, \mathbf{v})$ and $\mathbf{x} = \mathcal{I}(\mathbf{x}, \mathbf{v}_0)$ in to Equation 7, we can get

$$\delta\mathcal{L} = |\mathcal{L}(\mathcal{I}(\mathbf{x}, \mathbf{v}), \mathbf{y}) - \mathcal{L}(\mathcal{I}(\mathbf{x}, \mathbf{v}_0), \mathbf{y})|. \quad (8)$$

Approximating the loss function around \mathbf{v}_0 by the first-order Taylor expansion and ignoring the higher order terms, we can get

$$\mathcal{L}(\mathcal{I}(\mathbf{x}, \mathbf{v}), \mathbf{y}) = \mathcal{L}(\mathcal{I}(\mathbf{x}, \mathbf{v}_0), \mathbf{y}) + \nabla_{\mathbf{v}_0}\mathcal{L} \cdot (\mathbf{v} - \mathbf{v}_0), \quad (9)$$

where $\nabla_{\mathbf{v}_0}\mathcal{L}$ is a short form for $\nabla_{\mathbf{v}}\mathcal{L}(\mathcal{I}(\mathbf{x}, \mathbf{v}), \mathbf{y})|_{\mathbf{v}=\mathbf{v}_0}$.

Substituting it into Equation 8 gives

$$\delta\mathcal{L} = |\nabla_{\mathbf{v}_0}\mathcal{L} \cdot (\mathbf{v} - \mathbf{v}_0)| \leq \|\nabla_{\mathbf{v}_0}\mathcal{L}\|_q \cdot \|\mathbf{v} - \mathbf{v}_0\|_p, \quad (10)$$

where the Hlder inequality is used and $\frac{1}{p} + \frac{1}{q} = 1$.

The proposed method reduces the impact of input disturbance on the output by adding the flow gradients $\|\nabla_{\mathbf{v}_0}\mathcal{L}\|_q$ as a penalty term to the loss function, and the total loss is

$$Loss = \mathcal{L}(\mathbf{x}, \mathbf{y}) + \lambda \cdot \|\nabla_{\mathbf{v}_0}\mathcal{L}(\mathcal{I}(\mathbf{x}, \mathbf{v}), \mathbf{y})\|_q^2, \quad (11)$$

where λ is a hyperparameter specifying the penalty strength, and we set $p = q = 2$ in the following experiments.

FGR versus IGR

Next we explore the relationship between input gradients $\|\nabla_{\mathbf{x}}\mathcal{L}(\mathbf{x}, \mathbf{y})\|_q$ and flow gradients $\|\nabla_{\mathbf{v}_0}\mathcal{L}\|_q$. According to the chain rule, $\|\nabla_{\mathbf{v}_0}\mathcal{L}\|_q$ can be written as

$$\|\nabla_{\mathbf{v}_0}\mathcal{L}\|_q = \|\nabla_{\mathbf{x}'}\mathcal{L}(\mathbf{x}', \mathbf{y}) \cdot \nabla_{\mathbf{v}_0}\mathcal{I}(\mathbf{x}, \mathbf{v})\|_q. \quad (12)$$

Since $\nabla_{\mathbf{x}'}\mathcal{L}(\mathbf{x}', \mathbf{y})$ is equivalent to $\nabla_{\mathbf{x}}\mathcal{L}(\mathbf{x}, \mathbf{y})$ in input gradient regularization, we can get

$$\begin{aligned} \|\nabla_{\mathbf{v}_0}\mathcal{L}\|_q &= \|\nabla_{\mathbf{x}}\mathcal{L}(\mathbf{x}, \mathbf{y}) \cdot \nabla_{\mathbf{v}_0}\mathcal{I}(\mathbf{x}, \mathbf{v})\|_q \\ &\leq \|\nabla_{\mathbf{x}}\mathcal{L}(\mathbf{x}, \mathbf{y})\|_q \cdot \|\nabla_{\mathbf{v}_0}\mathcal{I}(\mathbf{x}, \mathbf{v})\|_q. \end{aligned} \quad (13)$$

Considering the derivative part, \mathcal{I} satisfies Lipschitz constraint, that is, the norm of the derivative of \mathcal{I} is bounded. Let $C = \sup_{\mathbf{x}} \|\nabla_{\mathbf{v}_0}\mathcal{I}(\mathbf{x}, \mathbf{v})\|_q$, then

$$\|\nabla_{\mathbf{v}_0}\mathcal{L}\|_q \leq C \cdot \|\nabla_{\mathbf{x}}\mathcal{L}(\mathbf{x}, \mathbf{y})\|_q. \quad (14)$$

Substitute it into equation 10

$$\begin{aligned} \delta\mathcal{L} &\leq \|\nabla_{\mathbf{v}_0}\mathcal{L}\|_q \cdot \|\mathbf{v} - \mathbf{v}_0\|_p \\ &\leq C \cdot \|\nabla_{\mathbf{x}}\mathcal{L}(\mathbf{x}, \mathbf{y})\|_q \cdot \|\mathbf{v} - \mathbf{v}_0\|_p, \end{aligned} \quad (15)$$

which means that $\|\nabla_{\mathbf{v}_0}\mathcal{L}\|_q$ is a tighter bound than $\|\nabla_{\mathbf{x}}\mathcal{L}(\mathbf{x}, \mathbf{y})\|_q$. Therefore, theoretically, regularizing $\|\nabla_{\mathbf{v}_0}\mathcal{L}\|_q$ can better resist adversarial deformations.

In fact, $\nabla_{\mathbf{v}_0}\mathcal{I}(\mathbf{x}, \mathbf{v})$ models the pointwise slope.

Random Start Technique

A drawback is that $\|\nabla_{\mathbf{v}}\mathcal{L}\|_q$ is undefined at the intersection, as an example shown in Figure 4. One consequence is, once the \mathbf{v}_0 is determined, $\|\nabla_{\mathbf{v}_0}\mathcal{L}\|_q$ is a constant, so it cannot reflect the characteristic of piecewise linear. To alleviate this problem, we add a random noise to \mathbf{v}_0 , make it able to cross the undefined point. An example of the problem and random start technique (RS) is shown in Figure 4.

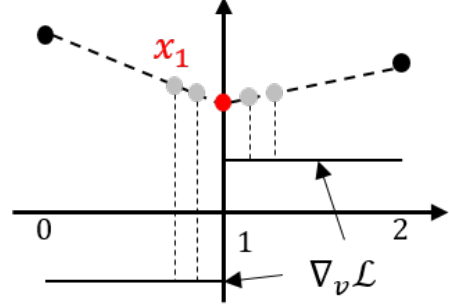


Figure 4: An example of random start technique used in this paper.

The total loss with FGR and RS is

$$Loss = \mathcal{L}(\mathbf{x}, \mathbf{y}) + \lambda \cdot \|\nabla_{\mathbf{v}_0+r}\mathcal{L}(\mathcal{I}(\mathbf{x}, \mathbf{v}), \mathbf{y})\|_q^2, \quad (16)$$

where $r \sim \mathcal{N}(0, \sigma^2)$ is a random noise.

Experiments

Setup

We conduct experiments on CIFAR-10, CIFAR-100 (Krizhevsky and Hinton 2010) and MNIST (LeCun et al. 1990) using VGG-11 (Simonyan and Zisserman 2014) and ResNet-18 (He et al. 2016). For all experiments, we use SGD optimizer with momentum of 0.9 and weight decay of $5e-4$. The batch size is set to 256, and the initial learning rate is 0.1. For MNIST, the learning rate is dropped by 10 every 10 epochs, and for CIFAR-10, CIFAR-100, it is dropped by 10 after 40 and 60 epochs. The total training duration is 30 and 80 epochs respectively. We employ random cropping as data augmentation, and all pixels are normalized to [0-1]. Besides, for CIFAR-10 and CIFAR-100, we also use random flipping with probability set to 0.5.

All experiments are implemented with PyTorch (Paszke et al. 2017) and run on a GeForce GTX 1080 Ti.

Attacks

All trained models are evaluated against adversarial deformations generated by four methods: single-step attack, multi-step attack, optimization-based attack, and gradient-free attack. Single-step and multi-step attacks are extending FGSM (Goodfellow, Shlens, and Szegedy 2014) and PGD (Madry et al. 2017) respectively. For the optimization-based attack, we adopt stAdv (Xiao et al. 2018b), and solve the problem with SGD. Evolution strategies (ES) (Rechenberg 1978) is used in gradient-free attack to find a suitable \mathbf{v} that fools DNNs.

Defenses

To test the proposed method, the following defenses are used to train a deep model:

- Standard, training without any defense methods;
- AT-FGSM, adversarial training with examples generated by l_∞ -bounded FGSM (Goodfellow, Shlens, and Szegedy 2014), and setting ϵ to 0.1 for MNIST, 0.01 for CIFAR-10 and CIFAR-100;
- AT-PGD, adversarial training with examples generated by l_∞ -bounded PGD (Madry et al. 2017), and setting ϵ to 0.1 for MNIST, 0.01 for CIFAR-10 and CIFAR-100, the number of iterations is 7;
- IGR, training with input gradient regularization (Ross and Doshi-Velez 2018), and setting λ to $\{1000, 3000, 5000, 7000\}$ for all datasets;
- FGR, training with flow gradient regularization, and setting λ to $\{100, 400, 500, 1000\}$ for all datasets;
- FGR+RS, training with flow gradient regularization and random start, and setting the standard deviation σ of the normal distribution to 0.01;
- FGR+RS+AT-PGD, combining FGR+RS and AT-PGD.

It should be noted that the selection of the above parameters, one part is to refer to the previous literature (Goodfellow, Shlens, and Szegedy 2014; Madry et al. 2017), such as 7 iterations for AT-PGD, and the other part is to ensure that all methods can acquire similar accuracy on clean images for a fair comparison.

Results

Our experimental results on CIFAR-10, CIFAR-100 and MNIST against different adversarial deformations are shown in Figure 6.

With similar accuracy on the clean set, training with FGR is significantly better than training with IGR when against adversarial deformations. Our results indicate, compared with IGR, FGR can bring additional adversary accuracy improvements in all cases, which are 0.2%-10.6%-32.7% (min-mean-max), 7.8%-16.2%-26.2%, and 4.4%-9.3%-18.9% on MNIST, CIFAR-10 and CIFAR-100 respectively. Similarly, the improvements under different attacks are 0.2%-7.0%-14.5%, 2.1%-9.3%-18.5%, 4.4%-16.5%-32.7% and 2.2%-15.2%-23.2% for single-step attack, multi-step attack, optimization-based attack and gradient-free attack respectively. Relatively speaking, FGR improves more on stronger adversarial attacks.

Random start can improve the effect of FGR without (or slightly) affecting the accuracy in clean images. In our experiments, the adversary accuracy improvements are -3.4%-3.2%-23.6%, 0.2%-3.7%-11.9%, 0.2%-2.8%-10.6% for MNIST, CIFAR-10 and CIFAR-100 respectively. For different attacks, the improvements are 0.2%-1.8%-5.8%, 0.3%-2.4%-6.8%, -0.2%-3.2%-23.6% and -3.4%-5.5%-14.9% for single-step attack, multi-step attack, optimization-based attack and gradient-free attack respectively. In all experiments, the average accuracy loss on clean images is 0.1%, which is almost negligible.

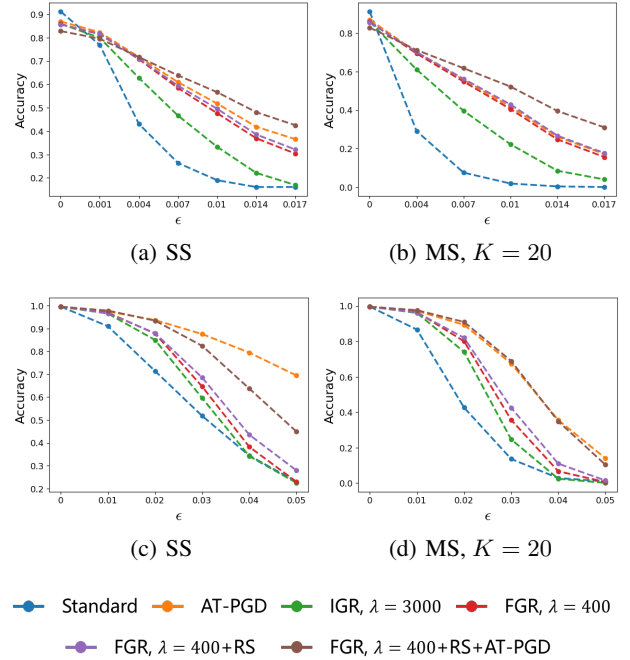


Figure 5: Performances of defenses in resisting single-step (SS) and multi-step (MS) attacks with different ϵ on CIFAR-10 and MNIST. (a)-(b): CIFAR-10, VGG-11. (c)-(d): MNIST, VGG-11. The results of CIFAR-100 are similar to CIFAR-10.

FGR and adversarial training have their own advantages. In general, adversarial training is better at resisting single-step and multi-step attacks, and models trained with FGR get stronger resistance to optimization-based and gradient-free attacks. We argue this is because in adversarial training, samples are generated through single-step or multi-step methods, so trained models will be somewhat “overfitting” to the two types of attack. Relatively, FGR belongs to gradient regularization and does not need to know in advance what optimization method to attack.

We count the number of optimal resistance obtained by different defense methods in Figure 6. For a fair comparison, for defenses with multiple instances, such as IGR and FGR, we select the point with the closest accuracy to AT-PGD on clean images. The results are shown in Table 1. Generally speaking, the combination of FGR+RS and AT-PGD can bring the best resistance to deep models.

In addition to the above experiments, we also test the performances of defense methods in resisting single-step and multi-step attacks with different budget ϵ , as shown in Figure 5. Consistent with previous observations, AT-PGD performs better than FGR when against single-step and multi-step attacks. Moreover, the gap between the two methods decreases as the number of iterations increases. Except for the single-step attack on MNIST, combining the two defenses can bring the best results.

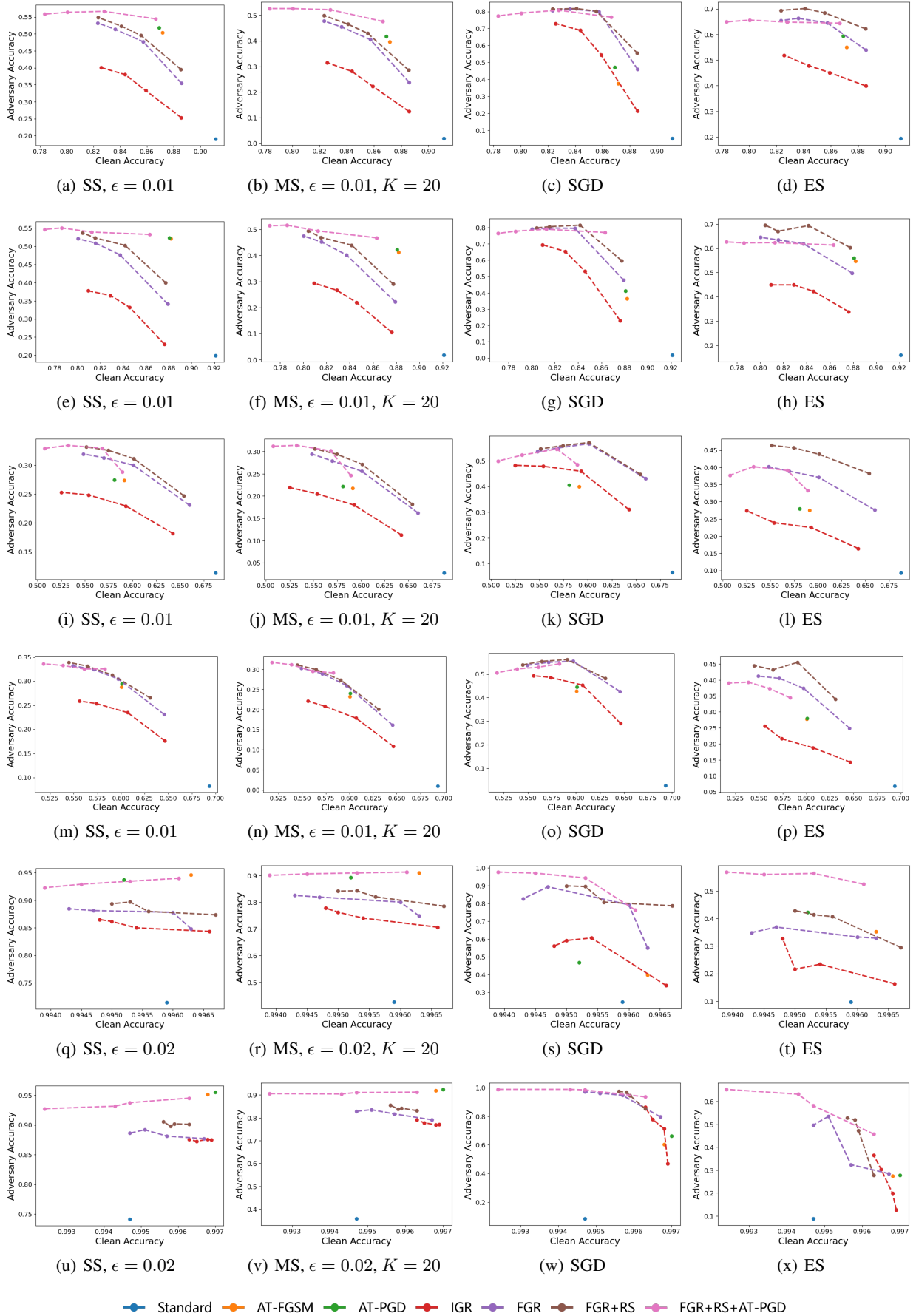


Figure 6: Results on CIFAR-10, CIFAR-100 and MNIST against adversarial deformations. (a)-(d): CIFAR-10, VGG-11. (e)-(h): CIFAR-10, ResNet-18. (i)-(l): CIFAR-100, VGG-11. (m)-(p): CIFAR-100, ResNet-18. (q)-(t): MNIST, VGG-11. (u)-(x): MNIST, ResNet-18. SS: single-step attack. MS: multi-step attack.

Table 1: Statistics of defenses that achieve the best resistance in the experimental results.

	MNIST	C10	C100	TOTAL
AT-FGSM	0	0	0	0
AT-PGD	3	0	0	3
IGR	0	0	0	0
FGR	0	0	0	0
FGR+RS	0	2	6	8
FGR+RS+AT-PGD	5	6	2	13

Loss Landscape

The classification loss values are computed along the adversarial flow direction and a random flow direction to analyze the loss landscape of the models trained with different defense methods, as shown in 7

Compared with standard training, both IGR, FGR and adversarial training can make the amplitudes lower. This shows that all defenses can reduce the sensitivity of models’ output to a small variation of input, and is consistent with the results in Figure 6.

However, the landscape changes in these defenses behave differently. Unlike FGR, where the landscape is almost smooth everywhere, the loss surface of IGR is still rugged in some areas. The main reason for this is that $\|\mathbf{x}' - \mathbf{x}\|_p$ is not entirely suitable for the variation generated by adversarial deformations. Random start can make the edge of FGR more smooth. In general, combining FGR and adversarial training can achieve the best results in both smoothness and amplitude.

Generalization of Gradient Regularization

Both FGR and IGR belong to the special form of gradient regularization. The main difference between them is how to measure the variation between adversarial examples and clean examples, where the former adopts $\|\mathbf{v} - \mathbf{x}_0\|_p$ and is designed for adversarial deformations, and the latter adopts $\|\mathbf{x}' - \mathbf{x}\|_p$ is designed for additive noise attacks.

But what should we do if encountering new types of attack? We discuss this important issue in this section. According to the above work and the observation of previous attacks, we try to expand IGR and FGR to a more general form. Many attacks, including additive noise and non-additive noise, can be represented into a unified form. Given a clean input image \mathbf{x} , the adversarial image \mathbf{x}' can be generated by $\mathbf{x}' = \tau(\mathbf{x}, \mathbf{n})$, where τ is a modification function, \mathbf{n} is the parameter of τ that controls the imposed change, \mathbf{n}_0 is the identity value so that $\mathbf{x} = \tau(\mathbf{x}, \mathbf{n}_0)$. Before showing how to represent different types of attack as τ , we first define some symbols for convenience:

- \mathcal{I} - bilinear interpolation function;
- \mathcal{A} - pointwise affine transformation function;
- \mathcal{G} - generative neural networks;
- \mathbf{m} - a mask of input image size.

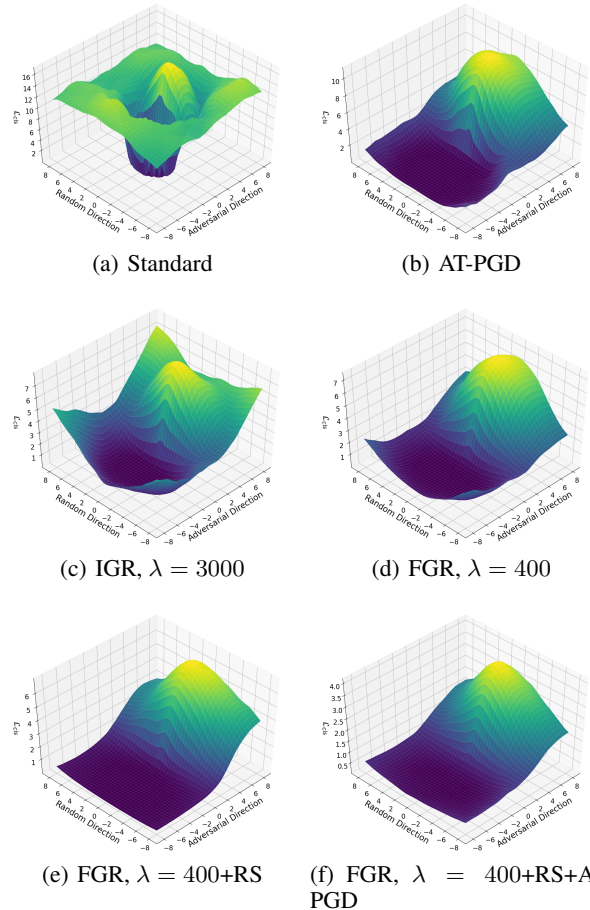


Figure 7: Loss surfaces along the adversarial flow and a random flow on CIFAR-10 with VGG-11.

Some forms of attack are summarized in Table 2.

After obtaining a unified form, substituting $\mathbf{x}' = \tau(\mathbf{x}, \mathbf{n})$ and $\mathbf{x} = \tau(\mathbf{x}, \mathbf{n}_0)$ into equation 7, we can get

$$\delta\mathcal{L} = |\mathcal{L}(\tau(\mathbf{x}, \mathbf{n}), \mathbf{y}) - \mathcal{L}(\tau(\mathbf{x}, \mathbf{n}_0), \mathbf{y})|. \quad (17)$$

Following similar steps as FGR, we can finally get a unified form of gradient regularization

$$Loss = \mathcal{L}(\mathbf{x}, \mathbf{y}) + \lambda \cdot \|\nabla_{\mathbf{n}_0} \mathcal{L}(\tau(\mathbf{x}, \mathbf{n}), \mathbf{y})\|_q^2, \quad (18)$$

where FGR and IGR are special forms when $\tau(\mathbf{x}, \mathbf{n}) = \mathcal{I}(\mathbf{x}, \mathbf{n})$, $\mathbf{n} = \mathbf{v}$ and $\tau(\mathbf{x}, \mathbf{n}) = \mathbf{x} + \mathbf{n}$, $\mathbf{n} = \delta$ respectively. For some other forms of attacks, the same method can be used to derive the corresponding regularization.

Conclusion

In order to increase the resistance of DNNs against adversarial deformations, a typical type of non-additive attacks, we propose a defense method named flow gradient regularization, which can model the characteristics of adversarial deformations. Besides, to better adapt to the piecewise linearity, we introduce a random start into flow gradient regularization.

Table 2: Summary of different forms of attack.

Methods	$\tau(\mathbf{x}, \mathbf{n})$	\mathbf{n}
Additive Noise Attacks (Madry et al. 2017; Carlini and Wagner 2017)	$\mathbf{x}' = \mathbf{x} + \mathbf{n}$	Additive Noise, δ
Multiplicative Noise Attack (Yang and Ji 2019)	$\mathbf{x}' = \mathbf{x} \cdot \mathbf{n}$	Multiplicative Noise
Adversarial Patches (Eykholt et al. 2018; Liu et al. 2018)	$\mathbf{x}' = \mathbf{x} + \mathbf{m} \cdot \mathbf{n}$	Additive Noise
Adversarial Deformations (Xiao et al. 2018b; Zhang and Wang 2019)	$\mathbf{x}' = \mathcal{I}(\mathbf{x}, \mathbf{n})$	Flow Matrix, \mathbf{v}
Affine Attacks (Engstrom et al. 2017; Zhao et al. 2019)	$\mathbf{x}' = \mathcal{I}(\mathbf{x}, \mathcal{A}(\mathbf{n}))$	Affine Matrix
Semantic Attacks (Joshi et al. 2019; Qiu et al. 2019)	$\mathbf{x}' = \mathcal{G}(\mathbf{x}, \mathbf{n})$	Attribute Vector

The proposed defenses are evaluated on MNIST, CIFAR-10 and CIFAR-100 against adversarial deformations generated by four methods, i.e., single-step attack, multi-step attack, optimization-based attack and gradient-free attack. The experimental results consistently show that, compared with IGR, models trained with FGR can get better resistance with a large margin. The comparison with adversarial training indicates that FGR is more suitable for resisting optimization-based and gradient-free attacks. Moreover, these two methods can be combined to improve models' robustness further.

Finally, a unified form of gradient regularization is discussed and both IGR and FGR are two special cases. Such a unified form can be used to derive the corresponding specific instance when facing other types of attack.

References

- [Afifi and Brown 2019] Afifi, M., and Brown, M. S. 2019. What else can fool deep learning? addressing color constancy errors on deep neural network performance. In *Proceedings of the IEEE International Conference on Computer Vision*, 243–252.
- [Alaifari, Alberti, and Gauksson 2018] Alaifari, R.; Alberti, G. S.; and Gauksson, T. 2018. Adef: an iterative algorithm to construct adversarial deformations. *arXiv preprint arXiv:1804.07729*.
- [Brown et al. 2017] Brown, T. B.; Mané, D.; Roy, A.; Abadi, M.; and Gilmer, J. 2017. Adversarial patch. *arXiv preprint 1712.09665*.
- [Carlini and Wagner 2017] Carlini, N., and Wagner, D. 2017. Towards evaluating the robustness of neural networks. In *2017 IEEE Symposium on Security and Privacy (SP)*, 39–57. IEEE.
- [Chan et al. 2019] Chan, A.; Tay, Y.; Ong, Y. S.; and Fu, J. 2019. Jacobian adversarially regularized networks for robustness. *arXiv preprint arXiv:1912.10185*.
- [Chen et al. 2017] Chen, P.-Y.; Zhang, H.; Sharma, Y.; Yi, J.; and Hsieh, C.-J. 2017. Zoo: Zeroth order optimization based black-box attacks to deep neural networks without training substitute models. In *Proceedings of the 10th ACM Workshop on Artificial Intelligence and Security*, 15–26.
- [Chen et al. 2018] Chen, P.-Y.; Sharma, Y.; Zhang, H.; Yi, J.; and Hsieh, C.-J. 2018. Ead: elastic-net attacks to deep neural networks via adversarial examples. In *Thirty-second AAAI conference on artificial intelligence*.
- [Croce and Hein 2019] Croce, F., and Hein, M. 2019. Minimally distorted adversarial examples with a fast adaptive boundary attack. *arXiv preprint arXiv:1907.02044*.
- [Croce and Hein 2020] Croce, F., and Hein, M. 2020. Reliable evaluation of adversarial robustness with an ensemble of diverse parameter-free attacks. *arXiv preprint arXiv:2003.01690*.
- [Dong et al. 2018] Dong, Y.; Liao, F.; Pang, T.; Su, H.; Zhu, J.; Hu, X.; and Li, J. 2018. Boosting adversarial attacks with momentum. In *Proceedings of the IEEE conference on computer vision and pattern recognition*, 9185–9193.
- [Engstrom et al. 2017] Engstrom, L.; Tsipras, D.; Schmidt, L.; and Madry, A. 2017. A rotation and a translation suffice: Fooling cnns with simple transformations. *arXiv preprint arXiv:1712.02779* 1(2):3.
- [Eykholt et al. 2018] Eykholt, K.; Evtimov, I.; Fernandes, E.; Li, B.; Rahmati, A.; Xiao, C.; Prakash, A.; Kohno, T.; and Song, D. 2018. Robust physical-world attacks on deep learning visual classification. In *Proceedings of the IEEE Conference on Computer Vision and Pattern Recognition*, 1625–1634.
- [Girshick 2015] Girshick, R. 2015. Fast r-cnn. In *Proceedings of the IEEE international conference on computer vision*, 1440–1448.
- [Goodfellow, Shlens, and Szegedy 2014] Goodfellow, I. J.; Shlens, J.; and Szegedy, C. 2014. Explaining and harnessing adversarial examples. *arXiv preprint arXiv:1412.6572*.
- [Gu and Rigazio 2014] Gu, S., and Rigazio, L. 2014. Towards deep neural network architectures robust to adversarial examples. *arXiv preprint arXiv:1412.5068*.
- [He et al. 2016] He, K.; Zhang, X.; Ren, S.; and Sun, J. 2016. Deep residual learning for image recognition. In *Proceedings of the IEEE conference on computer vision and pattern recognition*, 770–778.
- [Heaven 2019] Heaven, D. 2019. Why deep-learning ais are so easy to fool. *Nature* 574(7777):163.
- [Hein and Andriushchenko 2017] Hein, M., and Andriushchenko, M. 2017. Formal guarantees on the robustness of a classifier against adversarial manipulation. In *Advances in Neural Information Processing Systems*, 2266–2276.

- [Hoffman, Roberts, and Yaida 2019] Hoffman, J.; Roberts, D. A.; and Yaida, S. 2019. Robust learning with jacobian regularization. *arXiv preprint arXiv:1908.02729*.
- [Jakubovitz and Giryes 2018] Jakubovitz, D., and Giryes, R. 2018. Improving dnn robustness to adversarial attacks using jacobian regularization. In *Proceedings of the European Conference on Computer Vision (ECCV)*, 514–529.
- [Joshi et al. 2019] Joshi, A.; Mukherjee, A.; Sarkar, S.; and Hegde, C. 2019. Semantic adversarial attacks: Parametric transformations that fool deep classifiers. In *Proceedings of the IEEE International Conference on Computer Vision*, 4773–4783.
- [Kou et al. 2019] Kou, C.; Lee, H. K.; Chang, E.-C.; and Ng, T. K. 2019. Enhancing transformation-based defenses against adversarial attacks with a distribution classifier. In *International Conference on Learning Representations*.
- [Krizhevsky and Hinton 2010] Krizhevsky, A., and Hinton, G. 2010. Convolutional deep belief networks on cifar-10. *Unpublished manuscript* 40(7):1–9.
- [Krizhevsky, Sutskever, and Hinton 2012] Krizhevsky, A.; Sutskever, I.; and Hinton, G. E. 2012. Imagenet classification with deep convolutional neural networks. In *Advances in neural information processing systems*, 1097–1105.
- [Kurakin, Goodfellow, and Bengio 2016] Kurakin, A.; Goodfellow, I.; and Bengio, S. 2016. Adversarial machine learning at scale. *arXiv preprint arXiv:1611.01236*.
- [LeCun et al. 1990] LeCun, Y.; Boser, B. E.; Denker, J. S.; Henderson, D.; Howard, R. E.; Hubbard, W. E.; and Jackel, L. D. 1990. Handwritten digit recognition with a back-propagation network. In *Advances in neural information processing systems*, 396–404.
- [Liu et al. 2018] Liu, X.; Yang, H.; Liu, Z.; Song, L.; Li, H.; and Chen, Y. 2018. Dpatch: An adversarial patch attack on object detectors. *arXiv preprint arXiv:1806.02299*.
- [Long, Shelhamer, and Darrell 2015] Long, J.; Shelhamer, E.; and Darrell, T. 2015. Fully convolutional networks for semantic segmentation. In *Proceedings of the IEEE conference on computer vision and pattern recognition*, 3431–3440.
- [Lyu, Huang, and Liang 2015] Lyu, C.; Huang, K.; and Liang, H.-N. 2015. A unified gradient regularization family for adversarial examples. In *2015 IEEE International Conference on Data Mining*, 301–309. IEEE.
- [Madry et al. 2017] Madry, A.; Makelov, A.; Schmidt, L.; Tsipras, D.; and Vladu, A. 2017. Towards deep learning models resistant to adversarial attacks. *arXiv preprint arXiv:1706.06083*.
- [Paszke et al. 2017] Paszke, A.; Gross, S.; Chintala, S.; Chanan, G.; Yang, E.; DeVito, Z.; Lin, Z.; Desmaison, A.; Antiga, L.; and Lerer, A. 2017. Automatic differentiation in pytorch.
- [Qiu et al. 2019] Qiu, H.; Xiao, C.; Yang, L.; Yan, X.; Lee, H.; and Li, B. 2019. Semanticadv: Generating adversarial examples via attribute-conditional image editing. *arXiv preprint arXiv:1906.07927*.
- [Raghunathan, Steinhardt, and Liang 2018] Raghunathan, A.; Steinhardt, J.; and Liang, P. 2018. Certified defenses against adversarial examples. *arXiv preprint arXiv:1801.09344*.
- [Rechenberg 1978] Rechenberg, I. 1978. Evolutionsstrategien. In *Simulationsmethoden in der Medizin und Biologie*. Springer. 83–114.
- [Ross and Doshi-Velez 2018] Ross, A. S., and Doshi-Velez, F. 2018. Improving the adversarial robustness and interpretability of deep neural networks by regularizing their input gradients. In *Thirty-second AAAI conference on artificial intelligence*.
- [Ru et al. 2019] Ru, B.; Cobb, A.; Blaas, A.; and Gal, Y. 2019. Bayesopt adversarial attack. In *International Conference on Learning Representations*.
- [Sen, Ravindran, and Raghunathan 2020] Sen, S.; Ravindran, B.; and Raghunathan, A. 2020. Empir: Ensembles of mixed precision deep networks for increased robustness against adversarial attacks. *arXiv preprint arXiv:2004.10162*.
- [Shafahi et al. 2019] Shafahi, A.; Najibi, M.; Ghiasi, M. A.; Xu, Z.; Dickerson, J.; Studer, C.; Davis, L. S.; Taylor, G.; and Goldstein, T. 2019. Adversarial training for free! In *Advances in Neural Information Processing Systems*, 3353–3364.
- [Sharif et al. 2016] Sharif, M.; Bhagavatula, S.; Bauer, L.; and Reiter, M. K. 2016. Accessorize to a crime: Real and stealthy attacks on state-of-the-art face recognition. In *Proceedings of the 2016 acm sigsac conference on computer and communications security*, 1528–1540.
- [Sharif et al. 2017] Sharif, M.; Bhagavatula, S.; Bauer, L.; and Reiter, M. K. 2017. Adversarial generative nets: Neural network attacks on state-of-the-art face recognition. *arXiv preprint arXiv:1801.00349* 1556–6013.
- [Simon-Gabriel et al. 2019] Simon-Gabriel, C.-J.; Ollivier, Y.; Bottou, L.; Schölkopf, B.; and Lopez-Paz, D. 2019. First-order adversarial vulnerability of neural networks and input dimension. In *International Conference on Machine Learning*, 5809–5817.
- [Simonyan and Zisserman 2014] Simonyan, K., and Zisserman, A. 2014. Very deep convolutional networks for large-scale image recognition. *arXiv preprint arXiv:1409.1556*.
- [Song et al. 2018] Song, Y.; Shu, R.; Kushman, N.; and Ermon, S. 2018. Constructing unrestricted adversarial examples with generative models. In *Advances in Neural Information Processing Systems*, 8312–8323.
- [Su, Vargas, and Sakurai 2019] Su, J.; Vargas, D. V.; and Sakurai, K. 2019. One pixel attack for fooling deep neural networks. *IEEE Transactions on Evolutionary Computation* 23(5):828–841.
- [Szegedy et al. 2013] Szegedy, C.; Zaremba, W.; Sutskever, I.; Bruna, J.; Erhan, D.; Goodfellow, I.; and Fergus, R. 2013. Intriguing properties of neural networks. *arXiv preprint arXiv:1312.6199*.
- [Tramèr and Boneh 2019] Tramèr, F., and Boneh, D. 2019. Adversarial training and robustness for multiple perturba-

- tions. In *Advances in Neural Information Processing Systems*, 5858–5868.
- [Tramèr et al. 2017] Tramèr, F.; Kurakin, A.; Papernot, N.; Goodfellow, I.; Boneh, D.; and McDaniel, P. 2017. Ensemble adversarial training: Attacks and defenses. *arXiv preprint arXiv:1705.07204*.
- [Wang and Zhang 2019] Wang, J., and Zhang, H. 2019. Bilateral adversarial training: Towards fast training of more robust models against adversarial attacks. In *Proceedings of the IEEE International Conference on Computer Vision*, 6629–6638.
- [Xiao et al. 2018a] Xiao, C.; Li, B.; Zhu, J.-Y.; He, W.; Liu, M.; and Song, D. 2018a. Generating adversarial examples with adversarial networks. *arXiv preprint arXiv:1801.02610*.
- [Xiao et al. 2018b] Xiao, C.; Zhu, J.-Y.; Li, B.; He, W.; Liu, M.; and Song, D. 2018b. Spatially transformed adversarial examples. *arXiv preprint arXiv:1801.02612*.
- [Xie et al. 2017] Xie, C.; Wang, J.; Zhang, Z.; Ren, Z.; and Yuille, A. 2017. Mitigating adversarial effects through randomization. *arXiv preprint arXiv:1711.01991*.
- [Xu, Evans, and Qi 2017] Xu, W.; Evans, D.; and Qi, Y. 2017. Feature squeezing: Detecting adversarial examples in deep neural networks. *arXiv preprint arXiv:1704.01155*.
- [Yang and Ji 2019] Yang, X., and Ji, S. 2019. Learning with multiplicative perturbations. *arXiv preprint arXiv:1912.01810*.
- [Zhang and Wang 2019] Zhang, H., and Wang, J. 2019. Joint adversarial training: Incorporating both spatial and pixel attacks. *arXiv preprint arXiv:1907.10737*.
- [Zhang et al. 2019] Zhang, D.; Zhang, T.; Lu, Y.; Zhu, Z.; and Dong, B. 2019. You only propagate once: Painless adversarial training using maximal principle. *arXiv preprint arXiv:1905.00877 2*.
- [Zhao et al. 2019] Zhao, H.; Le, T.; Montague, P.; De Vel, O.; Abraham, T.; and Phung, D. 2019. Perturbations are not enough: Generating adversarial examples with spatial distortions. *arXiv preprint arXiv:1910.01329*.